A Collaborative Approach to Heading Estimation for Smartphone-based PDR Indoor Localisation

Marzieh Jalal Abadi*†, Luca Luceri‡*, Mahbub Hassan*†, Chun Tung Chou*, Monica Nicoli‡
*School of Computer Science and Engineering, University of New South Wales, Sydney, NSW 2052, Australia
Email: abadim, lucal, mahbub, ctchou@cse.unsw.edu.au
†National ICT Australia, Locked Bag 9013, Alexandria, NSW 1435, Australia
Email: Marzieh.Abadi, mahbub.hassan@nicta.com.au
‡Dipartimento di Elettronica, Informazione e Bioingegneria (DEIB), Politecnico di Milano, Italy
Email: luca.luceri@mail.polimi.it, monica.nicoli@polimi.it

***Abstract*—Pedestrian dead reckoning (PDR) is widely used for indoor localisation. Its principle is to recursively update the location of the pedestrian by using step length and step heading. A common method to estimate the heading in PDR is to use magnetometer measurements. However, unlike outdoor environments, the Earth's magnetic field is strongly perturbed inside buildings making the magnetometer measurements unreliable for heading estimation. This paper presents a new method to reduce heading estimation errors when magnetometers are used. The method consists of two components. The first component uses a machine learning algorithm to detect whether a heading estimate is within a specific error margin. Only heading estimates within the error margin are retained and passed to the second component, while the other estimates are discarded. The second component uses data fusion to average the heading estimates from multiple people walking in the same direction. The rationale of this component is based on the observation that magnetic perturbations are often highly localised in space and if multiple people are walking in the same direction, then only some of their magnetometers are likely to be perturbed. Data fusion between users can be carried out in a distributed manner by using a consensus algorithm with information sharing over wireless links. We tested the performance of our method using 92 datasets. The method is shown to provide an average heading estimate error of approximately 2°, which is more than 6-fold lower than the error of the heading estimate based only on raw magnetometer measurements (without any filtering and fusion). Assuming highly accurate step-length observation, the improved heading estimation leads to an average localisation accuracy of 55cm, which is an 80% improvement over PDR localisation using only raw magnetometer measurements.**

I. Introduction

Indoor localisation has many applications, such as location enabled services, indoor navigation, emergency response and many others. Although many network-based techniques have been proposed for indoor localisation [1], [2], they require infrastructure support which may not be always available, such as in emergency situations. Pedestrian Dead Reckoning (PDR) is an infrastructure-free localisation method which determines the position of people using inertial sensors, such as accelerometers, gyroscopes and magnetometers. The principle of PDR is to update the position of the subject after a step has been taken. The update can be performed recursively using the last known position, the step length and the estimated heading. The step length can be estimated relatively accurately [3], however the estimation of heading in the indoor environment is highly problematic. Gyroscope and magnetometer are typically employed for this purpose: the former can be used for a short time as it accumulates errors, while the magnetic field is highly perturbed in indoor environments due to structural elements of the building, electric systems, industrial and electronic devices [4]. A number of methods have been proposed to address the problem of heading estimation. For example, Kalman filter (KF) is used in [5] to fuse measurements from gyroscope and magnetometer so as to increase the heading estimation accuracy, whereas methods [1], [6], [7] exploit the magnetic field or WiFi fingerprinting to improve the location estimate.

In this paper, we propose a *self-contained* method, which uses only magnetometer measurements to reduce the heading estimation error. The method consists of two components. The aim of the first one is to detect whether a heading estimate obtained from the magnetometer measurements is within a specific error threshold. We show that this detection can be performed by machine learning using magnetometer measurements alone. Only the heading estimates that are selected as reliable by the detector are retained and passed to the second component. This other component exploits the observation that magnetic perturbation can be highly localised in space to improve the heading evaluation by fusing estimates from multiple subjects [8]. We exploit consensus algorithms [9], [10] to perform the fusion in a distributed fashion.

The contributions of the paper are as follows:

- We performed experiments to measure the magnetic fields in several areas of the university campus. We used these datasets to analyse the impact of magnetic perturbation on heading estimation. The key conclusion is that heading errors are highly localised in space.
- We proposed to use machine learning to detect whether the magnetometer measurements would result in a heading estimate within an error threshold. This detection method is self-contained and uses only magnetometer measurements.
- Given that heading estimation error is highly localised in

The work of Monica Nicoli was supported by the national project Mobilitá Intelligente Ecosostenibile (MIE), funded by MIUR within the framework Cluster Tecnologico Nazionale.

space, we proposed to use consensus algorithms to fuse in a distributed way the heading estimates of multiple people walking in the same direction. The distributed fusion of heading observations from multiple people does not appear to have been explored before.

- We conducted 92 experiments to evaluate the performance of our method. The results exhibited an average heading estimation error of 2.06°. This is a 6-fold error reduction compared to the heading estimation error based only on raw magnetometer measurements, which was 12.63°. The performance gain in terms of localisation accuracy was 80%.

The rest of the paper is organised as follows. Section II reviews related works while Section III presents the concept of spatial diversity. The two components of the proposed method are described in Sections IV and V. Experimental evaluation is presented in Section VI and Section VII concludes the paper.

II. Related Works

Many of the existing indoor positioning methods rely on an infrastructure and need reference points for identifying user locations. They use RF beacon tags [11]–[13] to perform triangulation [14] or fingerprinting to match Wi-Fi RSS measurements [1], [6], GSM signals [15], geomagnetic field [7] or ambient measurements [16] with an a-priori map. The accuracy of the position estimate in these methods depends on the physical environment, the quality of the map database and on the matching algorithms.

PDR [17], [18] is an infrastructure-free method, which relies on inertial sensors to track pedestrians with step detection and step orientation. Heading estimation is the major challenge in PDR and different techniques have been developed to face intrinsic sensor errors. Gyroscope and magnetometer are integrated to improve the heading estimation accuracy but the former accumulates an error known as drift and can be used for a short time [5], the latter suffers from perturbation due to indoor environments [4]. Hybrid solutions exploit the combination of PDR and other technologies as WiFi [19]–[22] and UWB [23] in order to take advantage of both techniques. The main drawback of these approaches is that they mostly suffer from slow convergence and large cumulated errors which are detrimental to the time critical indoor missions. Combining PDR with proximity sensing via sound beaconing to estimate relative positions [24] or deriving proximity information from Bluetooth visibility of devices [25] enhance the quality of PDR too.

A variety of new applications that rely on indoor position information of mobile nodes are emerging and their performance can be significantly improved by using cooperative algorithms [26]. If we consider an indoor environment where infrastructure based localisation is not applicable, an efficient solution can be a collaborative approach where users participate in the localisation process and share location-related information in order to improve the positioning performance. The higher is the degree of cooperation, the larger is the amount of information available for the estimation and thus the accuracy obtained in the localisation of the users [27]. However privacy and node selection are critical issues that considerably affect the performance of this approach.

In CLIPS [28], each user has a RSS reference map to determine a set of feasible coordinates using Wi-Fi beaconing. Then users employ dead reckoning over a floor map to remove invalid candidates and share the estimated coordinates. This approach provides accurate localisation and much lower position fix delay compared with a non-collaborative scheme. The work [29] proposes a cooperative localisation algorithm assuming that each mobile node is equipped with a ranging device to allow TDoA (Time Difference of Arrival) distance measurement between mobile nodes. Exploiting the "stop-and-go" behaviour of mobile nodes each subject can estimate its position based on the estimated positions of neighbouring nodes that have remained in their previous positions. People-Centric Navigation (PCN) [30] utilises the feature of "group activity" for a collaborative PDR. Measuring mobile phone's acceleration, heading and RSS of Bluetooth radios, PCN detects similarity among subjects and corrects PDR traces of the group members. EZ [31] does not require any knowledge of the physical layout and any user participation for the localisation process. Each user collects and reports to a localisation server RSS measurements corresponding to APs of unknown locations. The server uses this data to learn the characteristics of the propagation environment and to localise the users with a genetic algorithm. The paper [32] presents a method that enables the Bluetooth usage for collaborative localisation. It allows detecting and correcting caching delays and time-synchronization errors by tracking pairwise clock offsets between neighbours. In [33] a Wi-Fi based indoor positioning system is integrated with a human-centric collaborative feedback model that adjusts the positioning results. The work [34] proposes a consensus-based approach for distributed localisation based on RSS peer-to-peer measurements. Consensus algorithm is designed so as to account for the different degree of reliability of the location information provided by different neighbouring nodes.

III. Understanding the Nature of Heading Estimation Error

This section aims to provide evidence that the heading estimation error is highly localised in space, as this property underpins the indoor localisation approach that will be presented in the following section.

We conducted an experiment in a 8.1m $\times$ 6.3m room. Magnetometer measurements were collected from 264 points arranged in a grid with a spacing of 45cm. For each point, a Samsung Galaxy S III phone was placed with a heading of $h_1 = 280°$. An app on the phone collected magnetometer measurements at 100Hz for 20 seconds. We repeated the same experiment with a different reference heading of $h_2 = 100°$.

After obtaining the magnetometer readings for both the reference headings, we computed for each grid point the heading estimate and the average estimation error by averaging the error over the samples. Figure 1 shows the heat map

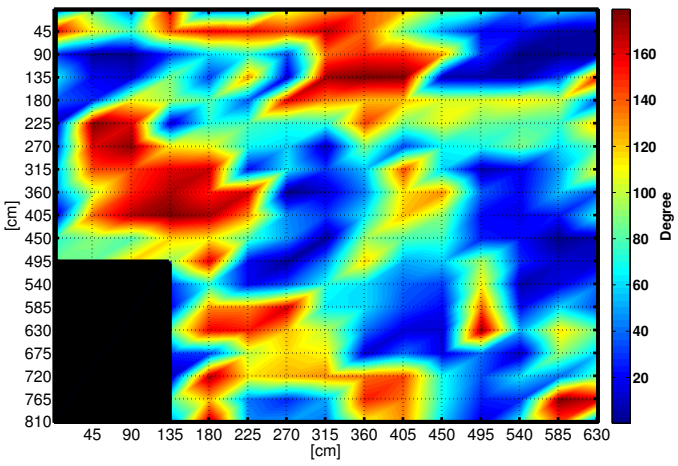

(a) True Heading=280°

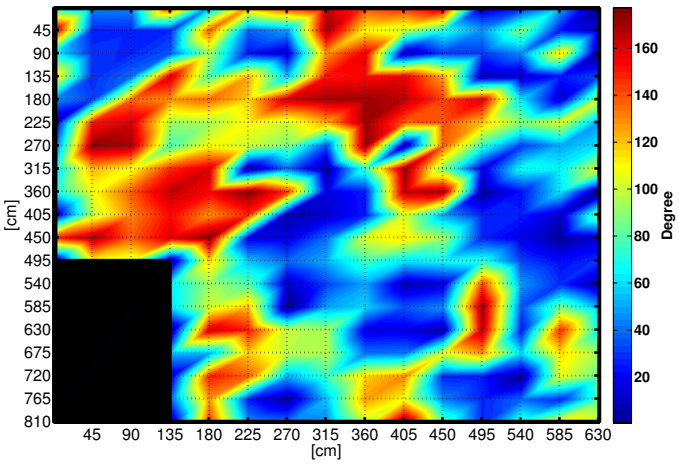

(b) True Heading=100°

Fig. 1: Heading Error Map. The black colour at the bottom left corner represents a space outside the room.

of estimation error for, respectively, the reference headings $h_1 = 280°$ and $h_2 = 100°$. The red and blue zones, indicate, respectively, areas of high and low estimation error. The black colour at the bottom left corner represents a space outside the room where no measurements were done. A few observations can be made: (1) Heading estimation error can be very high in some areas. (2) The two heat maps are fairly similar but the heading errors in two reference directions can be different at the same location. (3) The heading estimation error is rather localised with large values occurring at only certain pockets of space.

This indoor scenario was particularly challenging as the sensing devices (placed on the floor of the room) were highly disturbed and provided very noisy measurements resulting in some cases in extremely high estimate errors. Nevertheless, the interesting aspect is the highly localised nature of the heading error that is highlighted in the maps of Figure 1. This spatial diversity motivates us to investigate the fusion of multiple estimates from subjects walking in the same direction. Clearly, it is not desirable to include highly erroneous heading estimates in the fusion process, we therefore propose to detect these unreliable heading measurements and discard them before fusion is performed as discussed in the following section.

IV. Detecting Erroneous Heading Estimates

As mentioned earlier, our proposed system consists of two components. The first component detects erroneous heading estimates and the second component fuses heading estimates from multiple subjects.

The detection of the unreliable heading estimates is performed using as inputs the magnetometer measurements in the directions $\{x, y, z\}$ at time t, here denoted as $\{m_x(t), m_y(t), m_z(t)\}$.

The instantaneous heading of the subject at time t is computed as [35]:

$$h(t) = \tan^{-1}\left(\frac{m_y(t)}{m_x(t)}\right). \quad (1)$$

Magnetic perturbations in indoor environments may result in highly erroneous heading estimates. We propose to use machine learning to detect such unreliable estimates. Before describing the machine learning method, we first present the data collection campaign. Note that for brevity, we will drop the time index t from now onwards.

A. Data Collection Campaign

Magnetometer measurements were collected from 12 corridors in 6 buildings within the University of New South Wales campus in Sydney. Table I shows the experimental details. For some buildings, multiple corridors were selected from different floors or with different orientations, see Experiments 1 to 4 in Table I for example. The true heading for each direction of a corridor is identified from a map assuming that the corridor is parallel to the boundary walls of the building. We performed spatial sampling of the magnetic field by placing smartphones uniformly along the length of the corridor. The number of locations sampled in a corridor varied between 5 and 28, and the spacing between them varied from 2 to 3.9m, depending on the length of the corridor. At each location, magnetometer readings were recorded at 100Hz for 20 seconds.

B. Data Preprocessing

The machine learning algorithm used to detect erroneous headings relies on the fact that the Earth's main magnetic field can be assumed as stationary and known in a given area. We use the International Geomagnetic Reference Field (IGRF) [36] for Sydney as a reference. Each IGRF datum is a triplet (H, F, I) where H and F are respectively, the horizontal and total magnetic field, and I is the inclination

TABLE I: Experiment details, UNSW, Sydney

Dataset ID	Building (True Heading)	Number of locations	Spacing(m)
1	Electrical Engineering Building, Level 3 (99.20°)	16	3.30
2	Electrical Engineering Building, Level 3 (9.96°)	6	3.90
3	Electrical Engineering Building, Level 1 (99.20°)	18	2
4	Electrical Engineering Building, Level 1 (9.96°)	10	2
5	Robert Webster Building, Level 2 (189.96°)	5	2.50
6	Quantum Computation and Communication Technology Building, Ground Floor (9.09°)	17	2.20
7	School of Chemistry, Level 3 (279.05°)	5	2.30
8	School of Mathematics and Statistics, Level 1 (9.28°)	5	3.60
9	Burrows Theatre (156.80°)	7	2
10	School of Mathematics and Statistics, Level 2 (99.20°)	20	3
11	Robert Webster Building, Level 3 (189.7°)	13	3.30
12	Robert Webster Building, Level 3 (279°)	28	3.30

angle. These three quantities are related to the magnetic field strength $\{m_x, m_y, m_z\}$ at each point by:

$$F = \sqrt{m_x^2 + m_y^2 + m_z^2} \tag{2a}$$

$$H = \sqrt{m_x^2 + m_y^2} \tag{2b}$$

$$I = \tan^{-1}\left(\frac{m_z}{H}\right). \tag{2c}$$

Since the reference IGRF is known, we calculate the difference between the IGRF computed from measured magnetic field and the reference IGRF to obtain the error in the IGRF components F_{err}, H_{err} and I_{err}. We append these error figures to the raw magnetic field measurements to obtain a vector $\mathbf{M}$ with 6 elements:

$$\mathbf{M} = [m_x, m_y, m_z, F_{err}, H_{err}, I_{err}]. \tag{3}$$

We will refer to this as the *extended magnetic field measurement vector* $\mathbf{M}$.

C. Machine Learning

1) Time Window and Class Definition: Due to measurement errors, the instantaneous heading estimate fluctuates over time. Therefore, we propose to average the instantaneous heading estimates within a time window of 0.5s[2] to obtain a mean heading estimate $\bar{h}$. Let h_{true} be the true heading, the absolute heading error is $e = |\bar{h} - h_{\text{true}}|$. For a given threshold γ, we say that a mean heading $\bar{h}$ is *without perturbation* if $e \leq \gamma$, otherwise we say that it is *perturbed*. Formally, we define two classes C_0 and C_1. The class C_1 (resp. C_0) contains all the mean headings that are *without perturbation* (*perturbed*).

2) Feature Selection: Feature selection is an important step in machine learning [37]. Its aim is to select the features that are pertinent to accurately classifying the input data. We employ Correlation Feature Selection (CFS), which is a pre-processing step on the datasets to extract the important features to be used in model construction. By definition, a good feature subset is one that contains features highly correlated with (predictive of) the class, yet uncorrelated with (not predictive of) each other [38]. CFS exploits the information-theoretical concept of entropy to identify the best features.

We obtain our potential features using the following method. For each time window, we collect all the extended magnetic field measurement vectors $\mathbf{M}$ evaluated over the considered time interval. We then compute the 11 time-domain features listed in Table II for each element of $\mathbf{M}$. We thus get, for each time window, 66 different time domain features as $\mathbf{M}$ has 6 elements.

We apply CFS to all the 12 datasets listed in Table I using a threshold γ of 15°. The features selected by CFS for each dataset are given in Table III. Our observations and interpretations are:

- Each dataset has its own set of best features. In other words, there is not a common set of features that we can use for all datasets. This suggests that we are not able to use the same features for all the buildings. Moreover, this inference also holds for different corridors in the same building. These conclusions have also been confirmed by classification performance of machine learning algorithms and will be described in Section IV-C3. The previous observation is also consistent with the conclusions in Section III that heading estimation error is highly localised in space.
- Mean was most often the selected feature among all datasets.

Unfortunately CFS does not give us a common set of features that can be applied to all the datasets, but we really need that for our classification algorithm. We solve this impasse by selecting as features the means of the 6 elements of $\mathbf{M}$ over a time window. We will show in the following that this choice gives good classification accuracy.

3) Classification performance: We denote our choice of features for the time window j as $\bar{\mathbf{M}}_j = [\bar{m}_x, \bar{m}_y, \bar{m}_z, \bar{H}_{err}, \bar{F}_{err}, \bar{I}_{err}]$ where the bar denotes the mean quantity over the time window. For each time window, we determine whether the mean heading error is below the threshold γ or not. This allows us to label each mean heading estimate as class C_0 or C_1. Again, we use $\gamma = 15°$.

We use the following five classification algorithms for our evaluation: Support Vector Machine, Logistic Regression, Naïve Bayes, Decision tree and Multilayer Perceptron. The Weka [39] machine learning software is used for performance

[2]We used a time window of 0.5s because it is the average time to walk one step.

TABLE II: Time Domain Statistical Features

Feature	ME	LOBF	STD	ROC	MN	MX	R	MAD	RMS	SK	K
Definition	Mean	Slope of the Line of Best Fit	Standard deviation	Rate of Change	Minimum	Maximum	Range	Mean Absolute Deviation	Root Mean Square	Skewness	Kurtosis

TABLE III: Features selected by CFS method

Dataset ID	$\mathbf{m_x}$	$\mathbf{m_y}$	$\mathbf{m_z}$	$\mathbf{H_{err}}$	$\mathbf{F_{err}}$	$\mathbf{I_{err}}$
1		ME, RMS		ME, STD	ME	
2		ME, MX, MN	ME		ME	
3	ME	ME, RMS		MAD		MX
4	ME, RMS		RMS		STD	R
5	ME, RMS, MN					
6	ME, RMS	ME	SK			
7		ME			ME, MX, R	RMS
8			ME			RMS
9			RMS	ME, MX, MN		
10	ME	ME, MX, MN	MX		MN	R
11	ME, RMS	ME	ME			
12	ME	ME, RMS	ME	R		

analysis. For each dataset, we use 10-fold validation to create training and test sets. We report the classification results for each classifier and each dataset in Table IV. The deduction is that Logistic Regression performs the best since it has the highest average accuracy (98%) and the best worst case accuracy (90%).

The above results were obtained from using the model learnt from the training data in one corridor to classify test data of the same corridor. We have also attempted to build a model from data from a corridor in a building and test it on a different corridor in the same or different building. The classification accuracy for these tests for 4 different classification algorithms are reported in Table V. An observation is that the classification accuracy is much lower than those reported in Table IV. These results again confirm that we cannot build a general model that holds true for all the environments.

V. Distributed Fusion of Heading Estimates

In this section we propose to estimate the heading by fusing the measurements collected by N users in L time windows using a weighted average that accounts for the different degree of reliability of measurements. Only measurements retained by the first processing step are considered in the fusion. Fusion relies on the fact that the direction of walking is the same for the N users and it is slowly varying over time so that it can be assumed as constant in the considered time interval[3]. We denote the average heading estimate obtained by user $i = 1, \ldots, N$ in time window $j = 1, \ldots, L$ as $\bar{h}_{i,j} = h_{\text{true}} + w_{i,j}$ where h_{true} is the true heading and $w_{i,j}$ is the measurement error with variance $\sigma^2_{i,j}$. Fusion is conveniently applied to the Cartesian components $[\bar{x}_{i,j}, \bar{y}_{i,j}] = [sin(\bar{h}_{i,j}),\ cos(\bar{h}_{i,j})]$ rather than to the heading $\bar{h}_{i,j}$ directly, in order to avoid ambiguity problems in averaging angle measurements. Below we describe the fusion procedure that is used to draw the global estimate $\hat{x}$ from $\{\bar{x}_{i,j}\}$; a similar procedure is applied to $\{\bar{y}_{i,j}\}$ to get $\hat{y}$. The heading estimate is finally obtained as $\hat{h} = \tan^{-1}(\hat{x}/\hat{y})$.

We consider the fusion of the estimates $\bar{x}_{i,j}$ according to the Best Linear Unbiased Estimator (BLUE) [40]:

$$\hat{x} = \frac{\sum_{i=1}^{N}\sum_{j=1}^{L} \bar{x}_{i,j}/\sigma^2_{i,j}}{\sum_{k=1}^{N}\sum_{l=1}^{L} 1/\sigma^2_{k,l}}. \tag{4}$$

We propose to perform the above fusion as a cascade of two steps, fusion over time and fusion over users, as described in the following.

A. Fusion over Time

At first, each user performs a weighted average of the measurements collected in the L time windows as

$$\hat{x}_i = \frac{\sum_{j=1}^{L} \bar{x}_{i,j}/\sigma^2_{i,j}}{\sum_{k=1}^{L} 1/\sigma^2_{i,k}}. \tag{5}$$

Note that weighting by the variance inverse allows to account for the different degree of reliability at different windows. For practical implementation, the variances $\sigma^2_{i,j}$ are computed by users as sample variances from the measurements collected in window j.

B. Fusion between Users by Distributed Processing

The estimates obtained locally by the N users are merged as

$$\hat{x} = \sum_{i=1}^{N} \alpha_i \hat{x}_i, \tag{6}$$

[3]The assumption of constant or slow-varying heading is made according to the experiments carried out in this study where devices were moving always in the same direction. Adaptive filtering can be employed for data fusion in case of time varying heading.

TABLE IV: Comparison of classifiers

Dataset ID	Naive Bayes	Logistic	Multi Layer Perceptron	SVM	Decision Tree
1	97%	100%	81%	75%	90%
2	100%	100%	100%	100%	50%
3	89%	100%	89%	67%	92%
4	100%	100%	100%	60%	85%
5	80%	100%	60%	40%	50%
6	82%	94%	85%	76%	91%
7	60%	100%	100%	40%	40%
8	60%	100%	80%	80%	60%
9	85%	100%	100%	57%	78%
10	90%	90%	83%	60%	83%
11	92%	100%	85%	81%	73%
12	88%	96%	96%	69%	82%
Average accuracy	**82%**	**98%**	**88%**	**63%**	**71%**
Worst Case accuracy	**60%**	**90%**	**60%**	**40%**	**40%**

TABLE V: Classification accuracy when training and test data come from two different corridors

Training Dataset	Test Dataset	Naïve Bayes	Logistic	Multi Layer Perceptron	Decision tree
EE, Level 1 (99.20°)	EE, Level 3 (99.20°)	63%	69%	69%	56%
EE, Level 3 (9.96°)	EE, Level 1 (9.96°)	67%	67%	67%	67%
Robert Webster, Level 3 (189.7°)	Robert Webster, Level 2 (189.7°)	40%	80%	100%	80%
Robert Webster, Level 3 (279°)	Robert Webster, Level 3 (189.7°)	60%	60%	60%	60%
Mathematics, Level 1 (99.20°)	Mathematics, Level 1 (9.28°)	60%	50%	40%	60%

by a linear combination with weights $\{\alpha_i\}_{i=1}^N$. In order to guarantee the equality with (4), the weights must be set to $\alpha_i = \alpha_i^{\text{opt}} \triangleq \sigma_i^{-2}/(\sum_k \sigma_k^{-2})$, where σ_i^2 =var$(\hat{x}_i) = 1/\sum_j \sigma_{i,j}^{-2}$. We will consider both $\alpha_i = \alpha_i^{\text{opt}}$ and the simple average solution using $\alpha_i = 1$. For implementation of (6), we observe that our aim here is to develop an infrastructureless solution that can be exploited in all kinds of scenario: a central unit introduces costs and might be not available in certain environments or in case of disaster. Thereby, we propose to implement the fusion (6) by a distributed approach based on consensus [9], [10], [34]; this is an iterative process that consists on estimate exchanges on a peer-to-peer basis among the users of a network in order to reach a consensus for the evaluation of a certain quantity of interest [9]. The network in our scenario is the set of users that are walking in the same direction and have overcome the perturbation detector; we can model the network as a graph $\mathcal{G} = (\mathcal{V}, \mathcal{E})$ where the nodes $\mathcal{V} = \{1, ..., N\}$ are the users and the edges $\mathcal{E} \subseteq \mathcal{V} \times \mathcal{V}$ are the communication links among the nodes. Let $\mathbf{A} = [a_{ij}]$ be the $N \times N$ symmetric adjacency matrix, with $a_{ij} = 1$ if $(i, j) \in \mathcal{E}$ (i.e., if node j communicates with node i); $a_{ij} = 0$ for any $(i, j) \notin \mathcal{E}$. The neighbours of a user i are denoted by $\mathcal{N}_i = \{k \in \mathcal{V} : (i, k) \in \mathcal{E}\}$ and $d_i = |\mathcal{N}_i|$ is the node degree. The Laplacian matrix of the graph is $\mathbf{L} = \mathbf{D} - \mathbf{A}$ with $\mathbf{D} = \text{diag}(d_1, \ldots, d_N)$. In the consensus approach each node updates at each iteration its local estimate and exchanges it with its neighbours until an agreement is reached. At iteration n the estimate at user i is updated as follows:

$$\hat{x}_i(n+1) = \hat{x}_i(n) + \varepsilon W_i \sum_{k \in \mathcal{N}_i} (\hat{x}_k(n) - \hat{x}_i(n)), \tag{7}$$

where ε is the step size, selected as $0 < \varepsilon < 2/\lambda_{max}(\mathbf{W}^{-1}\mathbf{L})$, to guarantee convergence, with $\lambda_{max}(\cdot)$ denoting the maximum eigenvalue of the argument matrix and $\mathbf{W} = \text{diag}(W_1, \ldots, W_N)$ [10]. At step $i = 0$ the estimates are initialized as $\hat{x}_i(0) = \hat{x}_i$, i.e. each user utilises its own local estimate in the first iteration. According to [10], if weights W_i are chosen as $W_i = \sigma_i^2$ consensus converges to the global BLUE solution (4): $\hat{x}_i(\infty) = \hat{x}$. On the other hand if $W_i = 1$, consensus converges to (6) with $\alpha_i = 1/N$, i.e. to the average of the estimates at different users: $\hat{x}_i(\infty) = \frac{1}{N}\sum_{i=1}^N \hat{x}_i$. The two approaches are referred to as *weighted average consensus* (WAC) and *average consensus* (AC), respectively.

At the end of consensus processing the users that have taken part in the distributed algorithm spread the final estimate to the users that have been excluded by the perturbation detector. In this way we can take advantage from spatial diversity, since we need just one user with uncorrupted estimate in order to spread it to the other users. In the worst case scenario where all users do not overcome the perturbation detector (i.e., they all experienced bad measurements), users can employ their previous estimate as the current heading until at least one of them overcome the perturbation detector and spread the estimate to the others. If this scenario happens in the first time instant of the algorithm the users fuse their estimates even if they are all corrupted.

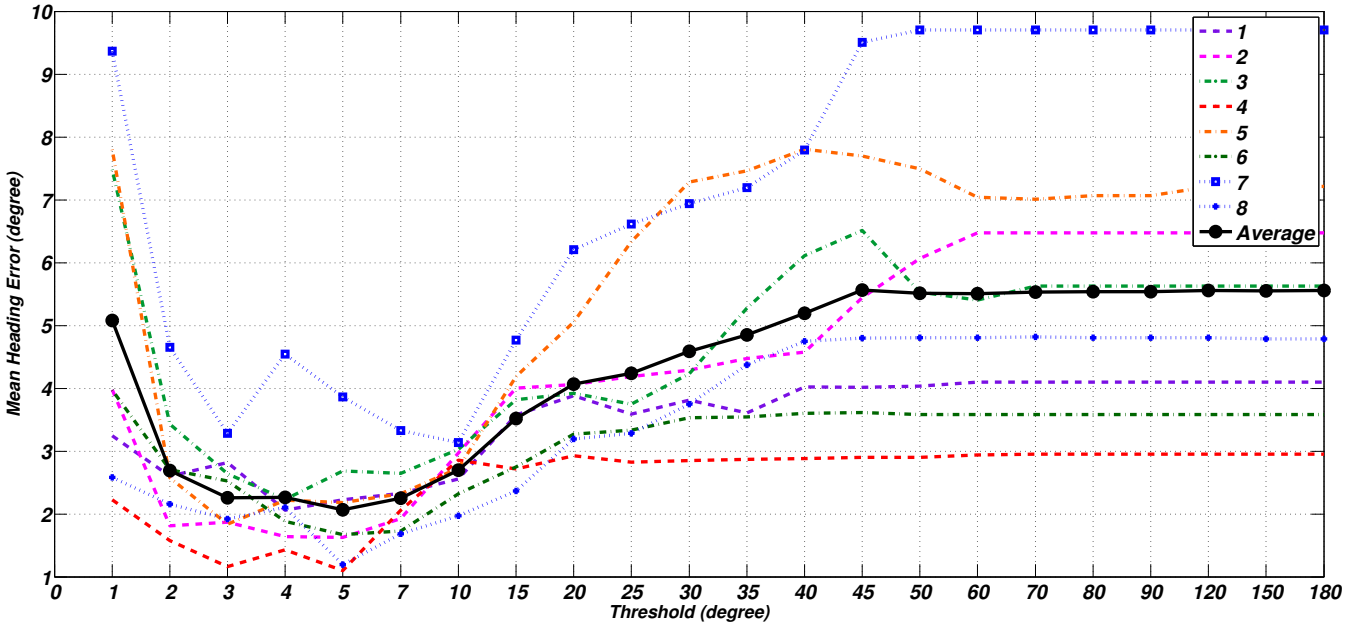

Fig. 2: Optimum Threshold

TABLE VI: Datasets for system evaluation

Scenario ID	UNSW Buildings	True heading	Number of Experiments
1	Library, 3rd Floor	188.98°	12
2	Old Main Building, Ground Floor	279.23°	12
3	Old Main Building, Ground Floor	99.46°	12
4	Robert Webster Building, LG Floor	99.26°	10
5	Robert Webster Building, LG Floor	279.18°	10
6	ABS Building, 1st Floor	99.26°	12
7	ABS Building, 1st Floor	279.15°	12
8	Electrical Engineering Building, 2nd Floor	98.90°	12

VI. Results and System Evaluation

In this section, we evaluate the performance of the proposed heading estimation algorithm using new experimental data. The details of the experimental scenario are described in Section VI-A. We then apply the algorithm and evaluate the performance in terms of heading estimation accuracy in Section VI-B. The localisation performance is studied in Section VI-C.

A. Testbed

In order to ensure diversity in environmental conditions, especially with respect to magnetic perturbation, experiments were conducted in 5 different buildings at University of New South Wales campus. One or two corridors were chosen from each of these buildings to create a set of experimental scenarios indexed from 1 to 8. The building names and the orientation of the corridor are summarised in Table VI. The true headings of the corridors were obtained from a map by assuming that the corridors are parallel to the boundary walls of the building. The number of experiments per scenario is indicated in the last column of Table VI. The total number is 92.

In each experiment, three subjects walked from one end to the other end of the chosen corridor. The three subjects started walking from the end of the corridor at different times. They followed lines on the flooring to walk in a straight line parallel to the corridor maintaining a separation of roughly 5m one another. The separation was selected so as to have a good chance of experiencing different degrees of perturbation at different users. Each subject carried either a HTC1X or HTC1X+ device in his hand and held the phone almost horizontally during the walk. We will refer to these three subjects by their position in the walk, as *Back*, *Middle* and *Front*. In order to minimise effects due to differences between people and between phone types, the subjects assumed different positions and held different phones in the different experiments. We used two different sampling frequencies, 16Hz and 50Hz for data collection.

B. Heading Accuracy

The heading error reduction provided by the proposed method strongly depends on the value of the threshold γ. We define the optimum threshold, γ^{opt}, as the threshold that minimises the heading error estimate. To find γ^{opt}, the heading estimate error is evaluated for several values of γ and for all the considered scenarios. The γ^{opt} is then selected as the one that minimises the average error for all scenarios. From Figure 2, it can be observed that for most of the scenarios, $\gamma^{\text{opt}} = 5°$ is the optimum threshold and for γ greater than 60°,

TABLE VII: Comparison of algorithms in terms of heading error (°)

Building (True Heading)	Raw PDR System	Perturbation Detector	WAC	AC	WAC & Perturbation Detector	AC & Perturbation Detector
Library (188.98°)	12.95	4.57	4.80	4.10	2.18	2.22
Old Main (279.23°)	12.91	7.99	10.29	6.47	2.31	1.63
Old Main (99.46°)	14.71	11.11	6.91	5.62	2.41	2.68
Robert Webster (279.18°)	10.34	3.56	5.54	2.80	1.00	1.04
Robert Webster (99.26°)	13.45	4.76	8.88	7.22	2.15	2.18
ASB (99.26°)	10.47	2.91	2.50	3.58	1.66	1.67
ASB (279.15°)	12.19	5.57	9.47	9.70	4.07	3.86
EE (98.90°)	14.15	4.25	7.32	4.78	1.23	1.19
Average Error	**12.65**	**5.59**	**6.96**	**5.53**	**2.13**	**2.06**

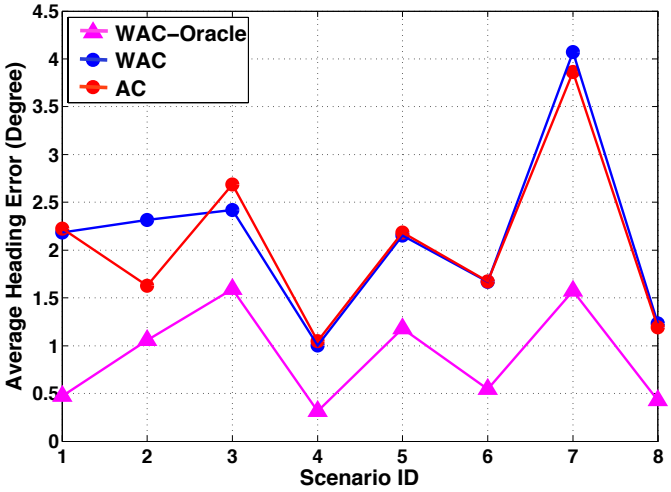

Fig. 3: Consensus Algorithm Comparison

the average error of fusion converges to the Naïve fusion value [8]; this is due to the fact that for large γ, all the measurements are assessed as data without perturbation and used for fusion. Another important observation from Figure 2 is that the value of the final heading estimate error for γ^{opt} is almost always less than 2.5° thanks to the fusion approach.

Table VII presents the performance of our technique for $\gamma^{\text{opt}} = 5°$ in case of window size equal to 8 samples for a 16Hz of sampling rate. The estimate with only perturbation detection is a simple average of the heading measurements. We observe that the average heading error over all experiments when we implement neither detector nor fusion (raw PDR) is 12.65°. Using only the perturbation detector reduces the average heading error to 5.59°(55.8% improvement), while using only the fusion components reduces the error to 5.53°(56.2%). However, when both the components are combined, we achieve a significant error reduction. The minimum average heading error is 2.06° (83.7%) achieved by the AC combined with the detector to filter perturbed data. The results obtained in all the experiments highlight that both the components are extremely important for the heading estimation.

Results in Table VII show that the performances of AC and WAC are similar. We would expect the WAC method to overcome the average consensus since WAC weights the estimates according to a reliability metric. To address this point, in Figure 3 we evaluate the performance of WAC using two different methods for weighting computation: in plain WAC, weights are computed using the sample variance of user i in window j as $\sigma^2_{i,j}$; in WAC-Oracle, the Mean Square Error (MSE) of the heading measurement is used in place of the sample variance, accounting also for bias. Note that WAC-Oracle requires the true heading to be available to calculate the MSE, hence the name Oracle. It can be seen that WAC-Oracle provides a performance gain over AC. Thereby, the main problem is related to the measurement bias that occurs in the selected scenarios and that is not accounted for in the weighting of BLUE (which assumes unbiased observations). A possible way to deal with this is performing first AC and then WAC using as reference for computing the weights the estimate at convergence of AC: the global average provided by AC can be used to identify and properly weight users affected by bias.

C. Localisation Accuracy

In this section, we investigate how the improvements in heading estimation increases the localisation accuracy of a given trajectory. We assume that heading and position are estimated at each pedestrian step. The average localisation accuracy, E, over the entire trajectory of M steps is obtained as the Root Mean Square Error (RMSE) of the position estimate as:

$$E = \sqrt{\frac{\sum_{i=1}^{M}(x_i - x'_i)^2 + (y_i - y'_i)^2}{M}} \tag{8}$$

where (x_i, y_i) is the true location and (x'_i, y'_i) is the location estimate for the i^{th} step.

In our experiments, the subjects were instructed to walk at a constant speed taking constant step lengths to the best of their abilities. The average walking speed was 1m/s and they were taking two steps per second on average. We, therefore, compute the heading estimate and update the new position every 0.5 seconds assuming a step length of 0.5m. For one of

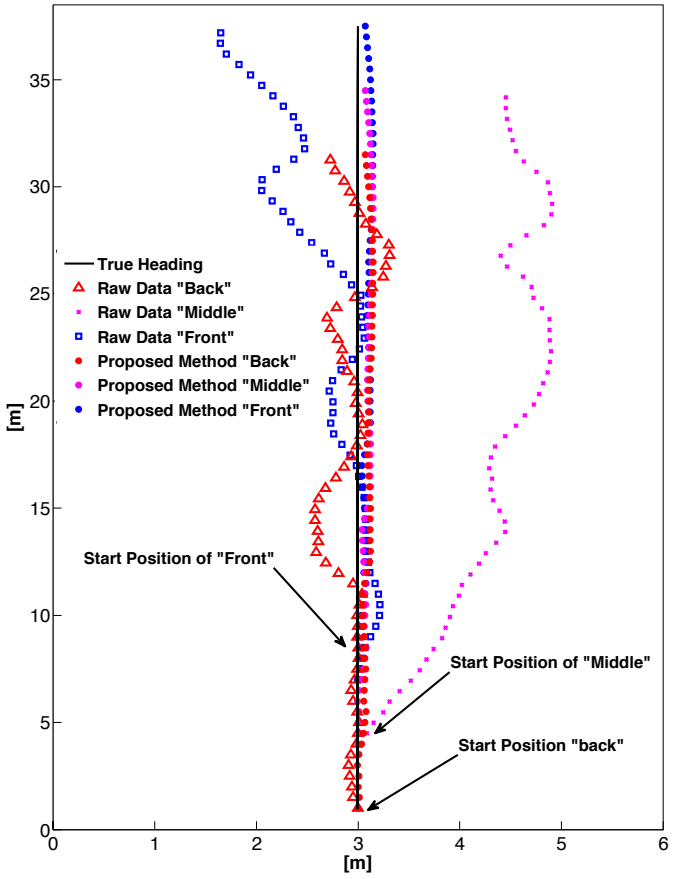

Fig. 4: Error Comparison in Old Main Building, (True Heading=279.23°)

the experiments, Figure 4 compares the position updates when the heading was estimated using the proposed method (circle markers) with the positions computed by individual heading estimates based on raw data without filtering and fusion (triangle, cross and square markers). The x-axis represents the width of the corridor while y-axis represents the length. As the three pedestrians walked one after the other, their starting positions were separated by roughly 5m along the length of the corridor.

In Figure 4, it is evident that the estimated positions are very close to the true when heading is estimated using the proposed method. For all experiments combined, the average localisation accuracy with the proposed heading estimate is 55cm, while individual estimates using raw PDR provide an average accuracy of 275cm. Therefore, for our data set, the proposed PDR method was able to improve the localisation accuracy by about 80%.

VII. Conclusion and Future Work

We have presented a new method for heading estimation in PDR making use of magnetometer measurements. Our method utilises two components in order to pre-filter perturbed measurements and fuse the data collected by multiple users to improve the heading estimate accuracy. We claim that just making use of one of the two components leads to an insufficient improvement in PDR localisation. In fact our system reaches an error reduction of 83.7% in the heading estimation and localisation error reduction of 80%.

In next step we will test our method in more dense networks comparing the performances and the communication costs. Furthermore the proposed system will be evaluated on real time data in more complex environments and paths. Future works will be addressed to further reduce the heading error associating other sensors to the magnetometer and exploiting new metrics for the WAC.

References

[1] P. Bahl and V. N. Padmanabhan, "RADAR: An in-Building RF-Based User Location and Tracking System," in *INFOCOM 2000. Nineteenth Annual Joint Conference of the IEEE Computer and Communications Societies. Proceedings. IEEE*, vol. 2. Ieee, 2000, pp. 775–784.

[2] E. Martin, O. Vinyals, G. Friedland, and R. Bajcsy, "Precise Indoor Localization using Smart Phones," in *Proceedings of the international conference on Multimedia*. ACM, 2010, pp. 787–790.

[3] F. Li, C. Zhao, G. Ding, J. Gong, C. Liu, and F. Zhao, "A Reliable and Accurate Indoor Localization Method using Phone Inertial Sensors," in *Proceedings of the 2012 ACM Conference on Ubiquitous Computing*. ACM, 2012, pp. 421–430.

[4] E. R. Bachmann, X. Yun, and A. Brumfield, "Limitations of Attitude Estimation Algorithms for Inertial/Magnetic Sensor Modules," *Robotics & Automation Magazine, IEEE*, vol. 14, no. 3, pp. 76–87, 2007.

[5] W. Geiger, J. Bartholomeyczik, U. Breng, W. Gutmann, M. Hafen, E. Handrich, M. Huber, A. Jackle, U. Kempfer, H. Kopmann *et al.*, "MEMS IMU for AHRS Applications," in *Position, Location and Navigation Symposium, 2008 IEEE/ION*. IEEE, 2008, pp. 225–231.

[6] M. Youssef and A. Agrawala, "The Horus WLAN Location Determination System," in *Proceedings of the 3rd international conference on Mobile systems, applications, and services*. ACM, 2005, pp. 205–218.

[7] J. Chung, M. Donahoe, C. Schmandt, I.-J. Kim, P. Razavai, and M. Wiseman, "Indoor Location Sensing using Geo-Magnetism," in *Proceedings of the 9th International Conference on Mobile systems, applications, and services*. ACM, pp. 141–154.

[8] M. J. Abadi, Y. Gu, X. Guan, Y. Wang, M. Hassan, and C. T. Chou, "Improving Heading Accuracy in Smartphone-based PDR Systems using Multi-Pedestrian Sensor Fusion," in *Proceeding of the 4th International Conference on Indoor Positioning and Indoor Navigation (IPIN13)*, Montbéliard-Belfort, France, 28-31 October 2013.

[9] R. Olfati-Saber, J. Fax, and R. Murray, "Consensus and Cooperation in Networked Multi-Agent Systems," *Proceedings of the IEEE*, vol. 95, no. 1, pp. 215–233, Jan 2007.

[10] M. Nicoli, G. Soatti, and S. Savazzi, "Distributed Estimation of Macroscopic Channel Parameters in Dense Cooperative Wireless Networks," *IEEE Wireless Communications and Networking Conference (WCNC)*, 6-9 April, Istanbul, Turkey 2014.

[11] J. Hightower, R. Want, and G. Borriello, "SpotON: An Indoor 3D Location Sensing Technology Based on RF Signal Strength," *UW CSE 00-02-02, University of Washington, Department of Computer Science and Engineering, Seattle, WA*, vol. 1, 2000.

[12] L. M. Ni, Y. Liu, Y. C. Lau, and A. P. Patil, "LANDMARC: Indoor Location Sensing using Active RFID," *Wireless networks*, vol. 10, no. 6, pp. 701–710, 2004.

[13] A. Nemmaluri, M. D. Corner, and P. Shenoy, "Sherlock: Automatically Locating Objects for Humans," in *Proceedings of the 6th international conference on Mobile systems, applications, and services*. ACM, 2008, pp. 187–198.

[14] M. Nicoli, C. Morelli, and V. Rampa, "A Jump Markov Particle Filter for Localization of Moving Terminals in Multipath Indoor Scenarios," *IEEE Transactions on Signal Processing*, vol. 56, no. 8, pp. 3801–3809, 2008.

[15] V. Otsason, A. Varshavsky, A. LaMarca, and E. De Lara, "Accurate GSM Indoor Localization," in *UbiComp 2005: Ubiquitous Computing*. Springer, 2005, pp. 141–158.

[16] M. Azizyan, I. Constandache, and R. Roy Choudhury, "SurroundSense: Mobile Phone Localization via Ambience Fingerprinting," in *Proceedings of the 15th annual international conference on Mobile computing and networking*. ACM, 2009, pp. 261–272.

[17] U. Steinhoff and B. Schiele, "Dead Reckoning from the Pocket-an Experimental Study," in *Pervasive Computing and Communications (PerCom), 2010 IEEE International Conference on*. IEEE, 2010, pp. 162–170.

[18] O. Woodman and R. Harle, "Pedestrian Localisation for Indoor Environments," in *Proceedings of the 10th international conference on Ubiquitous computing*. ACM, 2008, pp. 114–123.

[19] T. King, S. Kopf, T. Haenselmann, C. Lubberger, and W. Effelsberg, "Compass: A Probabilistic Indoor Positioning System Based on 802.11 and Digital Compasses," in *Proceedings of the 1st international workshop on Wireless network testbeds, experimental evaluation & characterization*. ACM, 2006, pp. 34–40.

[20] F. Evennou and F. Marx, "Advanced Integration of WiFi and Inertial Navigation Systems for Indoor Mobile Positioning," *Eurasip journal on applied signal processing*, vol. 2006, pp. 164–164, 2006.

[21] H. Wang, H. Lenz, A. Szabo, J. Bamberger, and U. D. Hanebeck, "WLAN-Based Pedestrian Tracking using Particle Filters and Low-Cost MEMS Sensors," in *Positioning, Navigation and Communication, 2007. WPNC'07. 4th Workshop on*. IEEE, 2007, pp. 1–7.

[22] P. Coronel, S. Furrer, W. Schott, and B. Weiss, "Indoor Location Tracking using Inertial Navigation Sensors and Radio Beacons," in *The Internet of Things*. Springer, 2008, pp. 325–340.

[23] J. A. Corrales, F. Candelas, and F. Torres, "Hybrid Tracking of Human Operators using IMU/UWB Data Fusion by a Kalman Filter," in *Human-Robot Interaction (HRI), 2008 3rd ACM/IEEE International Conference on*. IEEE, 2008, pp. 193–200.

[24] I. Constandache, X. Bao, M. Azizyan, and R. R. Choudhury, "Did You See Bob?: Human Localization using Mobile Phones," in *Proceedings of the sixteenth annual international conference on Mobile computing and networking*. ACM, 2010, pp. 149–160.

[25] K. Kloch, P. Lukowicz, and C. Fischer, "Collaborative PDR Localisation with Mobile Phones," in *Wearable Computers (ISWC), 2011 15th Annual International Symposium on*. IEEE, 2011, pp. 37–40.

[26] N. Patwari, J. N. Ash, S. Kyperountas, A. O. Hero, R. L. Moses, and N. S. Correal, "Locating the Nodes: Cooperative Localization in Wireless Sensor Networks," *Signal Processing Magazine, IEEE*, vol. 22, no. 4, pp. 54–69, 2005.

[27] H. Yamaguchiy, T. Higuchi, and T. Higashino, "Collaborative Indoor Localization of Mobile Nodes," *ICMU2012*, 2012.

[28] Y. Noh, H. Yamaguchi, U. Lee, P. Vij, J. Joy, and M. Gerla, "CLIPS: Infrastructure-Free Collaborative Indoor Positioning Scheme for Time-Critical Team Operations," in *Pervasive Computing and Communications (PerCom), 2013 IEEE International Conference on*. IEEE, 2013, pp. 172–178.

[29] T. Higuchi, S. Fujii, H. Yamaguchi, and T. Higashinoz, "An Efficient Localization Algorithm Focusing on Stop-and-Go Behavior of Mobile Nodes," in *Pervasive Computing and Communications (PerCom), 2011 IEEE International Conference on*. IEEE, 2011, pp. 205–212.

[30] T. Higuchi, H. Yamaguchi, and T. Higashino, "Clearing a Crowd: Context-Supported Neighbor Positioning for People-Centric Navigation," in *Pervasive Computing*. Springer, 2012, pp. 325–342.

[31] K. Chintalapudi, A. Padmanabha Iyer, and V. N. Padmanabhan, "Indoor Localization without the Pain," in *Proceedings of the sixteenth annual international conference on Mobile computing and networking*. ACM, 2010, pp. 173–184.

[32] A. Barreira, P. Sommer, B. Kusy, and R. Jurdak, "Towards Collaborative Localization of Mobile Users with Bluetooth."

[33] Y. Luo, O. Hoeber, and Y. Chen, "Enhancing Wi-Fi Fingerprinting for Indoor Positioning using Human-Centric Collaborative Feedback," *Human-centric Computing and Information Sciences*, vol. 3, no. 1, pp. 1–23, 2013.

[34] G. Soatti, M. Nicoli, A. Matera, S. Schiaroli, and U. Spagnolini, "Consensus Algorithms for Distributed Localization in Cooperative Wireless Networks," *The Eleventh International Symposium on Wireless Communication Systems (ISWCS 2014)*, August 26-29 2014, Barcelona, Spain 2014.

[35] P. Kaniewski and J. Kazubek, "Integrated System for Heading Determination," *Acta Physica Polonica-Series A General Physics*, vol. 116, no. 3, p. 325, 2009.

[36] C. Finlay, S. Maus, C. Beggan, T. Bondar, A. Chambodut, T. Chernova, A. Chulliat, V. Golovkov, B. Hamilton, M. Hamoudi *et al.*, "International Geomagnetic Reference Field: the Eleventh Generation," *Geophysical Journal International*, vol. 183, no. 3, pp. 1216–1230, 2010.

[37] A. L. Blum and P. Langley, "Selection of Relevant Features and Examples in Machine Learning," *Artificial intelligence*, vol. 97, no. 1, pp. 245–271, 1997.

[38] M. A. Hall, "Correlation-Based Feature Selection for Machine Learning," Ph.D. dissertation, The University of Waikato, 1999.

[39] M. Hall, E. Frank, G. Holmes, B. Pfahringer, P. Reutemann, and I. H. Witten, "The WEKA Data Mining Software: an Update," *ACM SIGKDD explorations newsletter*, vol. 11, no. 1, pp. 10–18, 2009.

[40] S. M. Kay, *Fundamentals of Statistical Signal Processing*. Prentice Hall, 1993, vol. Vol-I Estimation Theory.